Influence of ground motion spatial variation in the seismic risk of a proposed inter-city railway

F.J.T. Bernales, P.A.Y. Selda & R.A.C. Luna
AMH Philippines Inc., Quezon City, Philippines.

ABSTRACT

Spatially distributed infrastructures, such as inter-city railways, cover a great spatial extent wherein several asset portfolio components are exposed to seismic hazards. These hazards may possibly lead to prolonged service disruptions, inflated repair costs, and other economic losses. Practitioners primarily look at design motions from seismic hazard maps—typically generated only using classical probabilistic seismic hazard analysis—to evaluate the seismic performance of selected critical locations. However, in evaluating the seismic risk of regional-scale systems, these mapped values may be inappropriate because they do not necessarily represent vector-valued intensities from actual earthquakes. Issues may arise when predicting the seismic hazard at multiple locations or vectors of intensity measures due to the spatial correlation and cross-correlation of ground motion observations. This paper aims to explore these issues through the seismic risk estimation while considering scenario earthquakes to generate ground motion fields across spatially distributed systems. These approaches are applied to a proposed inter-city railway in Luzon, Philippines that traverses a major fault zone at multiple locations. The paper also highlights the implementation of these approaches using geographic information system tools from hazard modelling up to the documentation of seismic damage or risk values at any location of interest along the railway. Key issues and suggestions on how to further improve the state of practice are also raised at the end of the paper.

1 INTRODUCTION

Railway networks that can carry both freight and passengers play an important role in economic development. Inter-city railways provide such service for traversed areas spanning several kilometres. However, for seismically active regions like the Philippines, this also means that the railway networks have higher exposure to seismic hazard from nearby earthquake generators with an accompanying increase in seismic risk—possibly leading to service disruptions, inflated repair costs, and other economic losses.

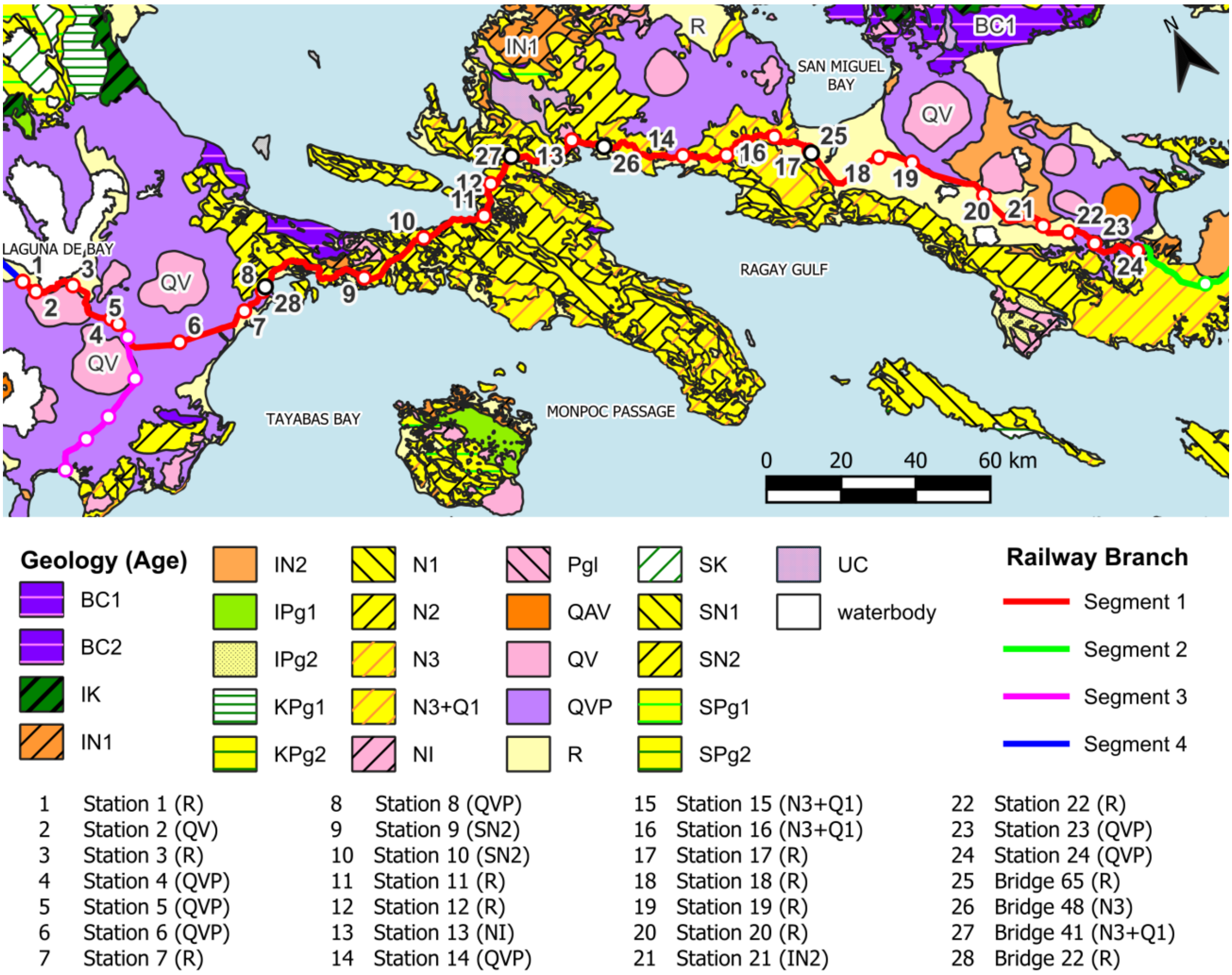

Figure 1: Location of railway stations and their corresponding geologic units. Railway branch segments are color-coded.

Transportation networks need to be assessed with the appropriate seismic hazard for each of its various interconnected components to insure its serviceability and safety. However, the current approach to evaluating the seismic hazard does not directly account yet for this interdependency. It normally generalizes the hazard characterization, quantified using an intensity measure (IM) for the entire system as if each will behave independently. As such, there is a need for an improved yet simple approach to account for the relationships across multiple IMs and for a spatial distribution of network assets or components.

This paper presents the application of the above concept and explores the seismic risk estimation while considering scenario earthquakes to generate ground motion fields (GMFs). These approaches are applied to a proposed inter-city railway in Luzon, Philippines (Figure 1) that traverses a major fault zone at multiple locations. The paper also highlights its implementation using geographic information system (GIS) tools from site characterization, hazard modelling, and up to the documentation of ground motion hazard values for stations of interest. Key issues and suggestions on how to further improve the state of practice and further applications in seismic risk assessment are also raised herein.

2 SITE CHARACTERIZATION

Local site conditions can have profound effects on all aspects (i.e. amplitude, frequency, and duration) of ground motions (Kramer 1996). As such, including site effects in ground motion models (GMMs) is a vital part of the seismic hazard characterization. Site effects in GMMs are typically calibrated using site proxies, such as the average shear wave velocity in the upper 30 m (V_{s30}) of a geologic profile, that can either be directly measured or correlated to regional or local geological data.

Downhole seismic tests (DST) were conducted in 20 locations along Segment 1, thereby providing direct V_{s30} measurements in each borehole (final depths > 30 m). Some test sites are in urban areas, so ambient and traffic vibrations could impact data quality. Despite these challenges, the recorded shear wave arrival can be distinctly recognized against the background noise with the help of standard signal processing techniques.

For sites without direct measurements, the V_{s30} can be inferred using regression equations (Akin et al., 2011; Brocher, 2008; Wair et al., 2012) and validated against the characteristics of local geologic units identified in regional geologic maps. GIS tools like QGIS (2023) can expedite this process by facilitating point classification using geologic unit background layers.

Figure 1 shows the locations of all the railways stations and bridges (numbered) superimposed with the geologic map. Moreover, the legend follows the Mines and Geosciences Bureau (MGB 2004) designations for the short names of the geologic units. Packages (or branching segments) are color-coded in the said figure, with the main and longest segment shown in red.

3 SEISMIC HAZARD EVALUATION

Once the site parameters are established, the seismic hazard can be evaluated using GMMs such as those developed from the NGA-West2 Project (Ancheta et al., 2014). However, practitioners still primarily look at design motions from seismic hazard maps—typically generated only using classical probabilistic seismic hazard analysis—to evaluate the seismic performance of selected critical locations or network segments. This section explores another approach in quantifying the location-specific seismic hazard: deterministic approach of considering scenario earthquakes to generate GMFs.

3.1 Earthquake Scenario

Deterministic seismic hazard analysis (DSHA) aims to quantify the effects of the ground motion intensity at a particular site based on a predefined scenario earthquake. With multiple uncertainties involved with earthquakes—such as its size (magnitude), location, and the ground shaking intensity—the resulting deterministic response spectra may be prudently taken as a single maximum envelope from each characteristic earthquake scenario considering all potential seismic sources.

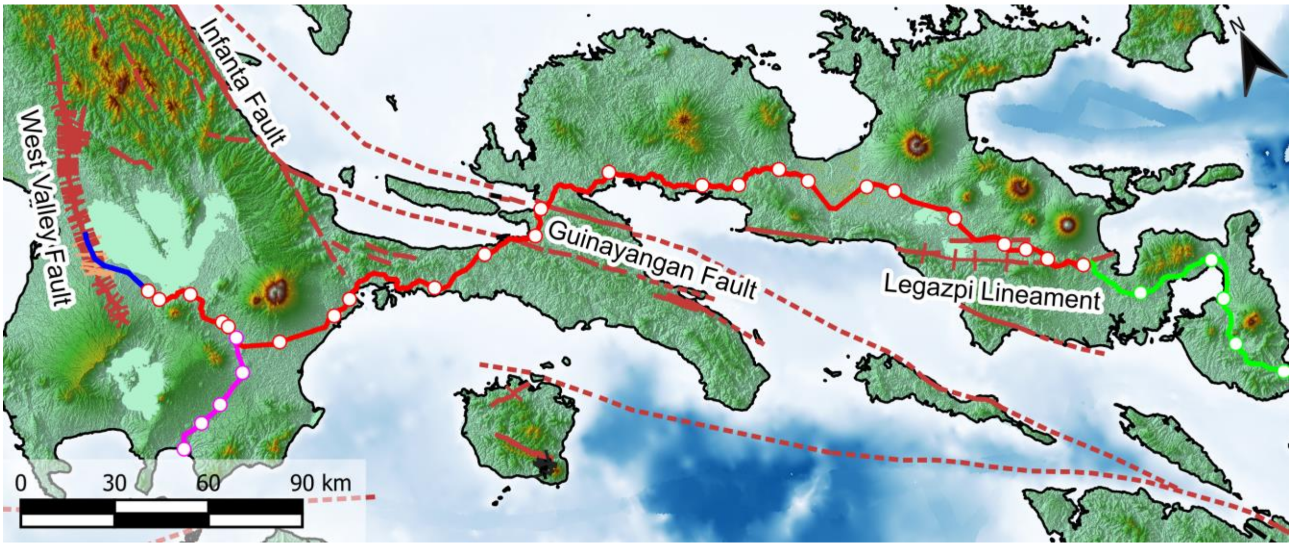

Figure 2: Relative locations of seismic sources considered in the study (Legazpi Lineament, West Valley, Guinayangan, and Infanta Faults) with respect to the railway line.

3.2 Ground Motion Values

The scenario-based seismic hazard analyses utilized the scenario hazard calculator of OpenQuake, an open-source seismic hazard and risk calculation software tool developed by the GEM Foundation (Pagani et al., 2014). All four NGA-West2 GMPEs (Abrahamson et al., 2014; Boore et al., 2014; Campbell & Bozorgnia, 2014; Chiou & Youngs, 2014) are applied, in equal weights (25% each), to the more critical fault sources in the vicinity of each site or station.

The seismological parameters corresponding to a full strike-slip rupture of the Legazpi Lineament (M_w 7.2), West Valley Fault (M_w 7.2), as well as the Guinayangan Fault (M_w 7.6) and Infanta Fault (M_w 7.6) segments of the Philippine Fault Zone were considered in the deterministic calculation (Figure 2). No calculations were done involving subduction zone earthquake scenarios as the source-to-site distances relative to the Philippine Trench make their deterministic estimates less significant compared to the said faults.

4 SPATIAL VARIABILITY AND CORRELATION OF GROUND MOTION HAZARD

When assessing seismic risk for spatially distributed systems with multiple dependent components, accounting for both cross-correlation and spatial correlation of ground motion is essential (Weatherill et al., 2013). The interdependence of infrastructure components and the correlation between spatial GMFs of different intensity measures from the same event cannot be overlooked. Therefore, a key challenge is to generate spatially correlated GMFs that accurately represent the underlying cross-correlation structure.

5 CASE STUDY

This section presents the application of seismic risk modelling to the inter-city railway in Luzon, Philippines. Shear wave velocity data were assigned to each railway station and bridge for site characterization, providing the basis for scenario-based ground motion hazard estimates given the four full strike-slip rupture scenarios defined earlier. Seismic risk calculations then incorporate exposure, fragility, and consequence models, which are detailed below.

5.1 Exposure Model

The location and geometry of the railway network were based on the proposed alignment agreed upon by project stakeholders at the time of writing. The exposure model includes railway stations and bridges identified as critical to the transportation system.

Information on additional facilities, such as maintenance, fuel, and dispatch centers, was unavailable at the time of writing and was therefore excluded. However, the framework remains flexible and modular, allowing for the incorporation of additional asset components as relevant data become available.

5.2 Fragility Model

Fragility functions, whether discrete or continuous, describe the probability of exceeding specific limit states given an intensity measure level. Often used as a hypernym, fragility functions herein result from the convolution of structural fragility and damage curves, bypassing the need for engineering demand parameters (EDPs). Since developing EDPs and fragility curves is beyond the scope of this work, fragility functions from the literature were adopted.

HAZUS (FEMA 2012) and SYNER-G (Argyroudis & Kaynia, 2014) provide fragility, damage, and loss functions for key infrastructure typologies, including bridges, buildings, lifelines, and transportation systems. Although the structural details of the railway bridges and station buildings remain uncertain at the time of writing, engineering design in the Philippines commonly follows American structural codes. Therefore, it is assumed that the fragility functions apply to the proposed railway system.

For risk calculations, four fragility functions—modelled as lognormal distributions with median values listed in Table 1—were considered. Railway track and station fragility functions are expressed in terms of peak ground acceleration (PGA), while bridge fragility functions are based on spectral acceleration at 1.0 sec, S_a(1.0s). Following HAZUS guidelines, standard deviations of 0.60 for seismically designed bridges, 0.64 for locally built steel light-frame railway stations, and 0.70 for railway tracks were adopted. The correlation between hazard and fragility due to local soil-structure interaction is assumed negligible, with site effects sufficiently accounted for through V_{s30}-scaling in the GMMs.

Table 1: Median values of the fragility models considered. Railway stations are in terms of PGA, while bridges are in terms of spectral acceleration at 1.0 s (Argyroudis & Kaynia, 2014; FEMA, 2012).

Damage Level	Railway Track	Railway Station	Single-span Bridge	Multi-span Minor Bridge	Multi-span Major Bridge
Slight	0.11	0.15	0.80	0.49	0.40
Moderate	0.18	0.26	1.00	0.60	0.50
Extensive	0.38	0.54	1.20	0.76	0.70
Complete	0.38	1.00	1.70	1.01	0.90

5.3 Consequence Model

Consequence models, represented as restoration curves, are used to evaluate economic or operational loss for each damage state. These curves describe the expected fraction of a component that remains operational over time following an earthquake. To estimate functional recovery times for railway system assets, the generic HAZUS functions were adopted. Likewise, it will be assumed that the consequence models also apply to the proposed railway system given the lack of region-specific data on recovery times.

It is important to note that multi-span major bridges inherently require longer recovery times than shorter bridges (Costa et al., 2016, 2018). However, the HAZUS recovery functions for railway bridges provide a single model regardless of bridge type. This assumption is not expected to significantly affect the results, as most of the bridges considered in this study are classified as major bridges.

6 RESULTS AND DISCUSSION

6.1 Damage Estimation

Damage levels for each rupture scenario were simulated using the Scenario Damage Calculator in OpenQuake v3.22. Figure 3 presents the median probability of collapse (i.e. complete damage) for all railway components considered. Box A corresponds to the Legazpi Lineament scenario, Box B to the West Valley Fault, Box C to the Guinayangan Fault, and Box D to the Infanta Fault. The corresponding fault rupture locations are also shown in Figure 3 for reference.

Clusters of high median collapse probability (up to 80%) are observed near the fault rupture traces. However, due to variations in fragility among railway components, not all are highly susceptible to extensive damage or collapse (see Box A). As a result, disruptions or losses may be localized rather than affecting the entire railway system.

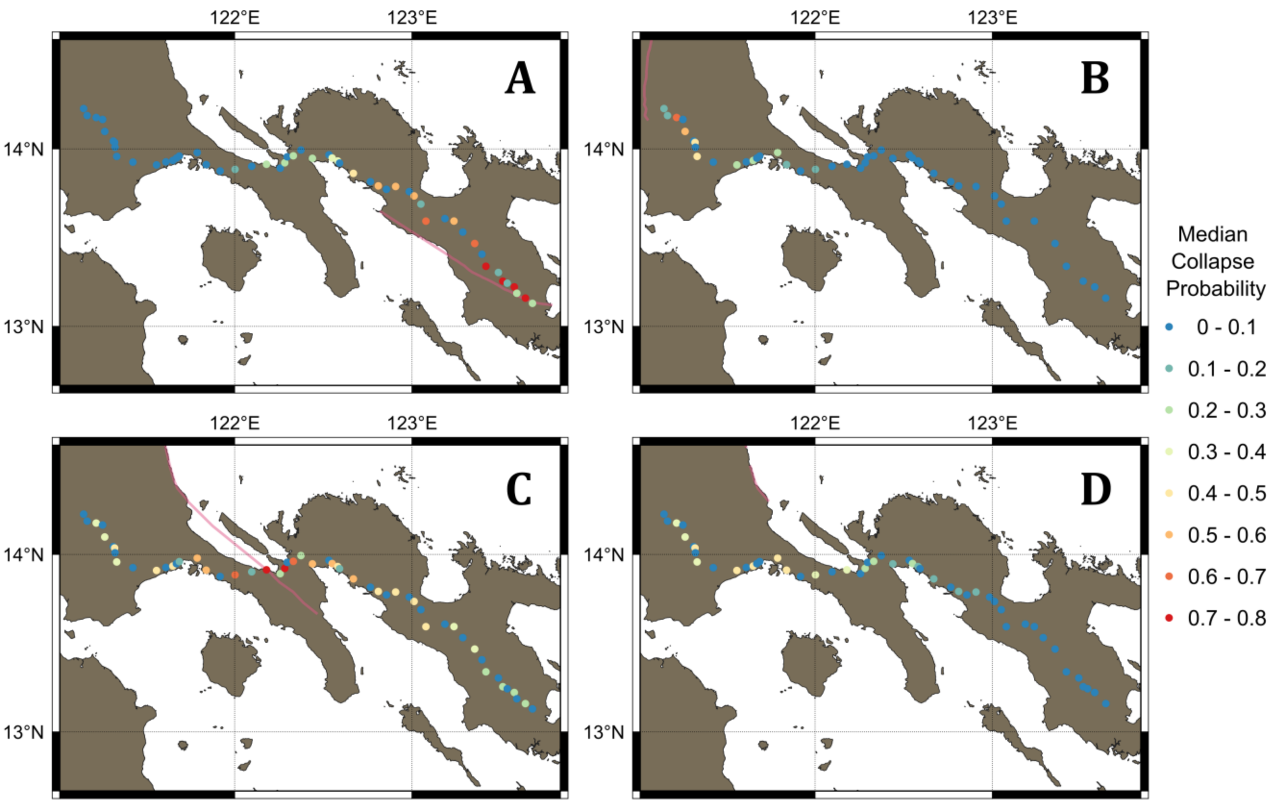

Figure 3: Median collapse (complete damage) probability along the railway segment.

6.2 Recovery Time Estimation

Recovery time accounts for all damaged components across various states—from minor damage to complete collapse. In contrast, disruption time may consider only the damage levels that render a path or segment impassable, such as extensive damage or collapse. Both metrics are highly influenced by the availability of resources following a seismic event.

If repairs are conducted sequentially, the total recovery time for a given path is the sum of the repair times for each affected asset along the route. However, when multiple bridges undergo repairs simultaneously, the total recovery time is significantly reduced, determined by the longest individual recovery time among the damaged structures.

Functional recovery time plays a crucial role in assessing indirect economic losses, as it directly impacts production downtime and the financial stability of the affected region.

6.3 Influence of Number of Ground Motion Fields

The scenario hazard described in Section 3 can be represented either by a single ground motion value (i.e. median) or a set of ground motion fields. While the median ground motion value may be useful in certain cases, GMFs provide a more comprehensive approach by accounting for inter- and intra-event variability as well as spatial correlation structures. Thus, it is essential to determine the minimum number of GMFs required to adequately capture uncertainty while maintaining computational efficiency.

Calculations indicate that the median intensity measures, represented by PGA and $S_a(1.0\text{s})$, converge significantly faster than the standard deviation. However, analysis suggests that 1,000 realizations are sufficient to ensure acceptable variation in both the mean and standard deviation (<10%). Based on these findings, 1,000 simulations were used to compute damage and risk metrics in this study.

6.4 Influence of Spatial Correlation

Spatially correlated GMFs generated by the same earthquake at different sites can significantly impact systemic and portfolio risk analysis (Weatherill et al., 2013). This study explores these effects through a parametric analysis comparing median, uncorrelated, and correlated GMFs and their influence on recovery time.

The ratio of disruption probabilities derived from uncorrelated and correlated GMFs is analyzed as a function of the shortest distance between adjacent railway components. As expected, the impact of spatial correlation on ground motion residuals—and consequently on disruption probabilities—diminishes with increasing distance, resulting in a ratio approaching one at larger separations.

Findings also indicate that relying solely on the median GMF underestimates disruption probabilities. Additionally, uncorrelated GMFs yield higher disruption probabilities compared to spatially correlated GMFs. This can be attributed to the increased likelihood of multiple assets experiencing severe or complete damage, as uncorrelated fields amplify the probability of localized high-intensity ground motion.

7 CONCLUSIONS

This study applies seismic risk estimation using scenario earthquakes to model spatially varying ground motion fields. These methods are implemented for a portfolio of railway assets associated with the proposed inter-city railway in Luzon, Philippines. Local site effects are characterized using geotechnical and geophysical data, while scenario hazard is assessed through empirical ground motion models. Exposure, fragility, and consequence functions are derived from HAZUS and SYNER-G models. Damage levels and restoration times are estimated for the railway components, with sensitivity analysis examining the effects of spatial correlation and number of ground motion fields.

Findings highlight that seismic hazard communication improves when seismic risk—expressed in terms of potential losses, downtime, and disruption—is quantified. Future research could explore event-based seismic risk analysis (Zhu et al., 2020) to incorporate probabilistic assessments over a defined investigation period or design/economic life.

ACKNOWLEDGMENTS

The authors extend their gratitude to other team members for their valuable contributions. Stanley Sayson aided in the seismic hazard modelling component. Ramon Quebral provided insightful advice on the structural geology aspects of this work. Lastly, we wish to thank Arlene Buenaventura-Paulino, Monica Baniquett-Panes—and most especially, Jenna Pallarca, for the leadership in project coordination.

REFERENCES

Abrahamson, N. A., Silva, W. J., & Kamai, R. (2014). Summary of the ASK14 Ground Motion Relation for Active Crustal Regions. *Earthquake Spectra*, *30*(3), 1025–1055. https://doi.org/10.1193/070913EQS198M

Akin, M. K., Kramer, S. L., & Topal, T. (2011). Empirical correlations of shear wave velocity (Vs) and penetration resistance (SPT-N) for different soils in an earthquake-prone area (Erbaa-Turkey). *Engineering Geology*, *119*(1–2), 1–17. https://doi.org/10.1016/j.enggeo.2011.01.007

Ancheta, T. D., Darragh, R. B., Stewart, J. P., Seyhan, E., Silva, W. J., Chiou, B. S.-J., Wooddell, K. E., Graves, R. W., Kottke, A. R., Boore, D. M., Kishida, T., & Donahue, J. L. (2014). NGA-West2 Database. *Earthquake Spectra*, *30*(3), 989–1005. https://doi.org/10.1193/070913EQS197M

Argyroudis, S., & Kaynia, A. M. (2014). Fragility Functions of Highway and Railway Infrastructure. In K. Pitilakis, H. Crowley, & A. M. Kaynia (Eds.), *SYNER-G: Typology Definition and Fragility Functions for Physical Elements at Seismic Risk* (Vol. 27, pp. 299–326). Springer Netherlands. https://doi.org/10.1007/978-94-007-7872-6_10

Boore, D. M., Stewart, J. P., Seyhan, E., & Atkinson, G. M. (2014). NGA-West2 Equations for Predicting PGA, PGV, and 5% Damped PSA for Shallow Crustal Earthquakes. *Earthquake Spectra*, *30*(3), 1057–1085. https://doi.org/10.1193/070113EQS184M

Brocher, T. M. (2008). Compressional and Shear-Wave Velocity versus Depth Relations for Common Rock Types in Northern California. *Bulletin of the Seismological Society of America*, *98*(2), 950–968. https://doi.org/10.1785/0120060403

Campbell, K. W., & Bozorgnia, Y. (2014). NGA-West2 Ground Motion Model for the Average Horizontal Components of PGA, PGV, and 5% Damped Linear Acceleration Response Spectra. *Earthquake Spectra*, *30*(3), 1087–1115. https://doi.org/10.1193/062913EQS175M

Chiou, B. S.-J., & Youngs, R. R. (2014). Update of the Chiou and Youngs NGA Model for the Average Horizontal Component of Peak Ground Motion and Response Spectra. *Earthquake Spectra*, *30*(3), 1117–1153. https://doi.org/10.1193/072813EQS219M

Costa, C., Silva, V., & Bazzurro, P. (2018). Assessing the impact of earthquake scenarios in transportation networks: The Portuguese mining factory case study. *Bulletin of Earthquake Engineering*, *16*(3), 1137–1163. https://doi.org/10.1007/s10518-017-0243-2

Costa, C., Vitor Silva, & Paolo Bazzurro. (2016). Assessing scenario seismic risk of transportation networks. *Portuguese Journal of Structural Engineering*, *3*(2), 23–32. https://doi.org/10.34638/RPEE-SIII-N02

Federal Emergency Management Agency (FEMA). (2012). *Hazus-MH 2.1—Earthquake model technical manual*. Department of Homeland Security, Washington.

Kramer, S. L. (1996). *Geotechnical earthquake engineering*. Prentice Hall.

Mines and Geosciences Bureau. (2004). *Geology and Mineral Resources of the Philippines*. Mines and Geosciences Bureau, Department of Environment and Natural Resources.

Pagani, M., Monelli, D., Weatherill, G., Danciu, L., Crowley, H., Silva, V., Henshaw, P., Butler, L., Nastasi, M., Panzeri, L., Simionato, M., & Vigano, D. (2014). OpenQuake Engine: An Open Hazard (and Risk) Software for the Global Earthquake Model. *Seismological Research Letters*, *85*(3), 692–702. https://doi.org/10.1785/0220130087

QGIS.org. (2023). *QGIS Geographic Information System* (Version 3.28.4-Firenze) [Computer software].

Wair, B. R., DeJong, J. T., & Shantz, T. (2012). *Guidelines for Estimation of Shear Wave Velocity Profiles* (No. PEER 2012/08). University of California, Berkeley.

Weatherill, G., Vitor Silva, Crowley, H., & Bazzurro, P. (2013). *Exploring Strategies for Portfolio Analysis in Probabilistic Seismic Loss Estimation*. https://doi.org/10.13140/2.1.3526.2720

Zhu, W., Liu, K., Wang, M., & Koks, E. E. (2020). Seismic Risk Assessment of the Railway Network of China's Mainland. *International Journal of Disaster Risk Science*, *11*(4), 452–465. https://doi.org/10.1007/s13753-020-00292-9